Journal of Fluorine Chemistry 131 (2010) 510–516

Contents lists available at ScienceDirect

Journal of Fluorine Chemistry

journal homepage: www.elsevier.com/locate/fluor

The relevance of the fluorine interactions in the supramolecular structure of a complex constructed from copper(II) hexafluoroacetylacetonate and the 4′-(3-pyridyl)-2,2′:6′,2″-terpyridine ligand. Novel C–F/π synthons involving the π-system of the terpyridine moieties and those of the hexafluoroacetylacetonate chelate rings

Juan Granifo [a,*], Dominique Toledo [a], María Teresa Garland [b], Ricardo Baggio [c]

[a] Departamento de Ciencias Químicas, Facultad de Ingeniería, Ciencias y Administración, Universidad de La Frontera, Temuco, Chile
[b] Departamento de Física, Facultad de Ciencias Físicas y Matemáticas and CIMAT, Universidad de Chile, Santiago de Chile, Chile
[c] Departamento de Física, Comisión Nacional de Energía Atómica, Buenos Aires, Argentina

ARTICLE INFO

Article history:
Received 7 October 2009
Received in revised form 28 October 2009
Accepted 30 October 2009
Available online 11 November 2009

Keywords:
Fluorine interactions
C–F···π interactions
Hexafluoroacetylacetonate
4′-(3-Pyridyl)-2,2′:6′,2″-terpyridine
Copper(II) complexes

ABSTRACT

Reaction of 4′-(3-pyridyl)-2,2′:6′,2″-terpyridine (pyterpy) with $Cu(hfacac)_2$ (hfacac = hexafluoroacetylacetonate) led to the formation of the novel compound $[Cu_3(hfacac)_4(\mu\text{-pyterpy})_2][Cu(hfacac)_3]_2$ (**1**). The structure is composed of a trinuclear $[Cu_3(hfacac)_4(\mu\text{-pyterpy})_2]^{2+}$ cation and two $[Cu(hfacac)_3]^-$ anionic species. The cation consists of a chain of three Cu^{II} atoms connected by bridging pyterpy ligands. The $[Cu(hfacac)_3]^-$ anions have the hfacac ligands coordinated in their usual chelating manner through their carbonyl O donors. Besides the coulombian forces, the ionic species are fixed by C–H···O, C–H···F, F···F and a variety of unusual inter-ion C–F···π interactions that control the packing motif. These π-interactions involve the terpyridine groups from the pyterpy ligand and the five-membered rings of the chelating hexafluoroacetylacetonate anions.

© 2009 Elsevier B.V. All rights reserved.

1. Introduction

Supramolecular chemistry is one of the most active areas of research in modern chemistry. The incorporation of new functional ligands such as 2,2′:6′,2″-terpyridine (terpy) and its derivatives into supramolecular assemblies by transition metal complexation, creating novel materials with useful chemical and physical properties, appears as one important challenge in this field [1,2]. In this sense, the pyridyl-substituted ligands 4′-(*n*-pyridyl)-terpyridine (*n* = 2, 3 or 4) have been studied and found that they can act as bridging N-donor ligands using its tridentate terpyridyl fragment and the monodentate *n*-pyridyl moiety [3–11]. In particular, only recently, the bridging mono-tridentate capacity of the 4′-(3-pyridyl)-2,2′:6′,2″-terpyridine (pyterpy, Scheme 1) ligand has been tested. More specifically, the reported examples showing this capacity appear in homometallic polymers [3–5], heterobimetallic polymers [6,7] and trinuclear heterobimetallic species [6]. Besides, solid state studies show that a significant group presenting weak intermolecular interactions is the one involving the pyterpy ligand in a π–π stacking between neighboring pyridyl rings [4,6]. We present herein the crystal and supramolecular structure of a novel complex, $[Cu_3(hfacac)_4(\mu\text{-pyterpy})_2][Cu(hfacac)_3]_2$ (**1**), with the pyterpy ligand connecting in a mono-tridentate way the metal centres of the cation component, producing a singular trinuclear homometallic unit. In this compound the usual π-stacking contacts involving the pyterpy ligand are not present, but instead, the presence of the CF_3 groups from the hfacac ligand allows a prominent intervention of the π-rings through a series of C–F···π(pyridyl, pyridyl-chelate or hfacac-chelate rings) interactions.

2. Results and discussion

2.1. Synthesis

Complex **1** was isolated by the reaction of an excess of $Cu(hfacac)_2{\cdot}H_2O$ with pyterpy in a dichloromethane solution. Slow evaporation of the solution at room temperature afforded dark green blocks suitables for single crystal X-ray analysis.

* Corresponding author. Tel.: +56 045 325434; fax: +56 045 325440.
E-mail address: jgranifo@ufro.cl (J. Granifo).

0022-1139/$ – see front matter © 2009 Elsevier B.V. All rights reserved.
doi:10.1016/j.jfluchem.2009.10.016

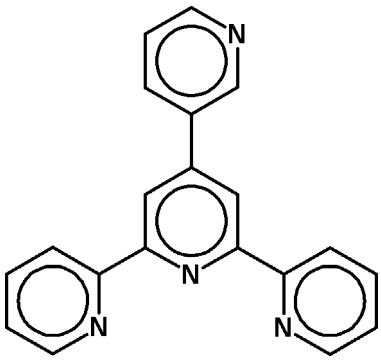

Scheme 1. Structure of the pyterpy ligand.

Table 1
Selected geometric parameters (Å) for **1**.

Cu1–O15	1.975(4)	Cu2–O24	2.170(4)
Cu1–N46	2.011(5)	Cu3–O23	1.952(4)
Cu1–O25	2.277(4)	Cu3–O12	1.981(4)
Cu2–N26	1.903(5)	Cu3–O13	1.986(4)
Cu2–O14	1.922(4)	Cu3–O21	2.006(5)
Cu2–N16	2.017(5)	Cu3–O11	2.219(5)
Cu2–N36	2.022(5)	Cu3–O22	2.228(4)

2.2. Coordination geometry and bonding

Fig. 1 shows a structural diagram of compound **1**, the core of the whole group is located in the central copper atom Cu1, which lays on a symmetry centre; as a result the independent unit is just one half of the reported formula. The trinuclear cationic species (which includes Cu1, Cu2 and Cu2^{i}, (i): $(1-x, 1-y, 1-z)$) evolves around the centrosymmetric octahedral Cu1 centre, to which the 3-pyridyl group of pyterpy (through its unique nitrogen atom N46) and a chelating hfacac (through O15 and O25) bind. The resulting octahedral geometry is rather regular, showing the usual Jahn–Teller distortion with the apical Cu1–O25 bond being 14% longer than the remaining two, very similar, basal ones (Table 1). Cu2, in turn, is pentacoordinated into the shape of a slightly distorted square pyramid, by the tridentate portion of the pyterpy (κ^3N,N′,N″) ligand and a chelating hfacac (κ^2O,O′). The least squares plane through the basal atoms (N16, N26, N36, O14) leaves the metal 0.22(1) Å away towards the apical direction, a line almost perpendicular to the base, only 6.8(1)° away from the plane normal. This "out-of-plane" positioning of the cation has the effect of forcing the terpyridyl core into a slightly concave shape by driving the three pyridilic rings significantly out of parallelism (dihedral angles between pyridil rings: (Py(N16), Py(N26): 9.4(1)°; Py(N36), Py(N26): 16.5(1)°). The fourth-pyridyl group, in turn is appreciably rotated around the C86–C166 bond (Py(N26), Py(N46): 32.1(1)°).

The mononuclear $[Cu(hfacac)_3]^-$ anionic part is built up around Cu3 (Fig. 1), which presents an octahedral coordination given by the six oxygen atoms from three chelating hfacac ligands. Its "propeller like" geometry does not differ from previously reported ones in other equivalent $[Cu(hfacac)_3]^-$ units [12], either in its coordination distances (including the Jahn–Teller axial deformation of a rather regular octahedral environment) or its interatomic angles. The similarities include the presence of far-from-negligible "slanting" angles (defining as such the "inclination" with which the ligand approaches the cation and measures by the dihedral angle subtended by the O–Cu–O coordination plane and the ligand mean plane) (range for **1**: 4.2(1)–25.2(1)°). These angles are usually significantly different from zero for $[Tr(hfacac)_3]^-$ units [13–16] but not, for instance, for their $[Tr(acac)_3]^-$ counterparts, where acac: acetylacetonato and the terminal groups are CH_3 [17–19]. It is tempting to ascribe the reasons behind these different behaviours to the intermolecular interactions to which the terminal CF_3 groups are involved, either as C–H···F, C–F···π or C–F···F–C, thus dragging the very labile ligand orientation out of their coordination planes, much in the way as a door is easily moved on its hinges (see Section 2.3.4).

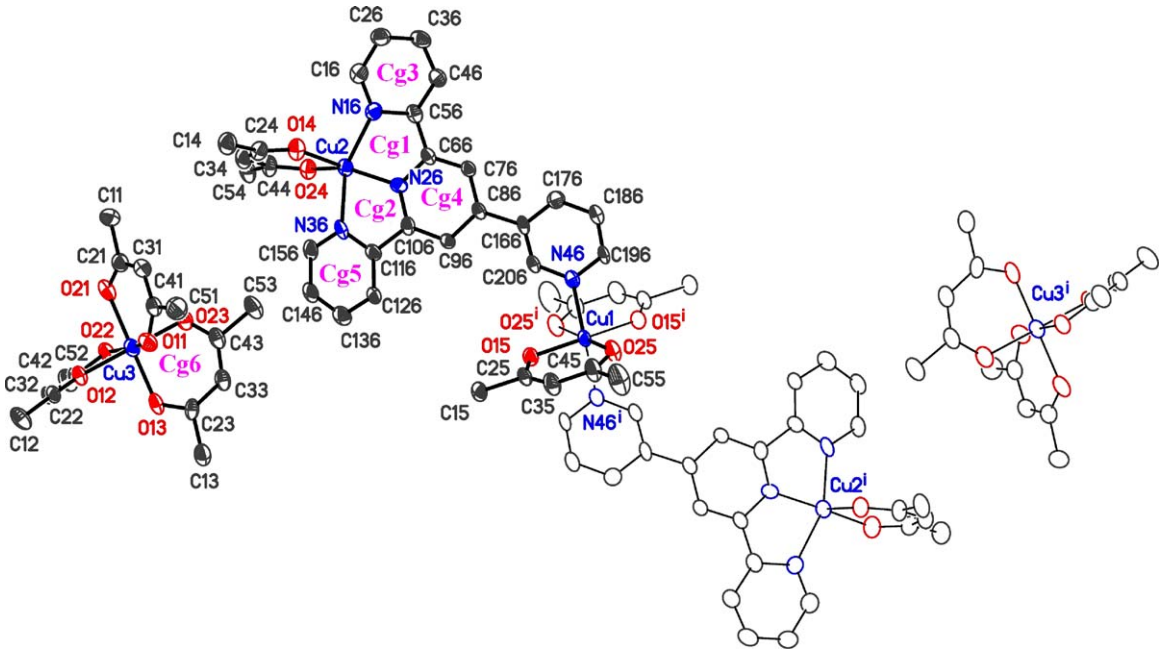

Fig. 1. Structural diagram of **1** showing the numbering scheme used, applied only to the independent part of the coordination polyhedron (drawn in full thermal ellipsoids and full bonds, at a 30% probability level). Fluorine and hydrogen atoms have been omitted for clarity. Cg(I) refers to the ring centre-of-gravity. Symmetry code: (i) $1-x, 1-y, 1-z$.

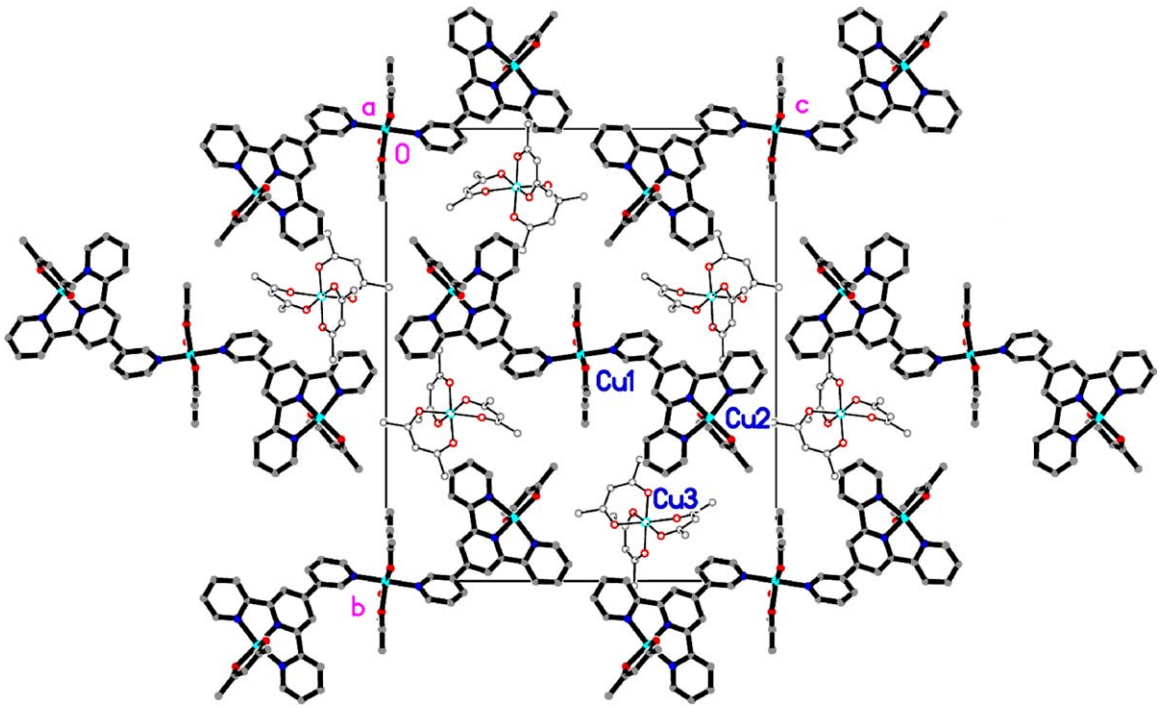

Fig. 2. Packing view of **1** along the *a*-axis showing the way in which ionic columns dispose. Cationic columns, in bold lining; anionic ones, in simple lining. For clarity, fluorine and hydrogen atoms have been omitted.

The coulombian forces arising between ions constitute the strongest and definitory stabilizing interactions. The effect of the latter is that both the anionic groups (centred at Cu3) and the cationic fragments (centred at Cu2, at both sides of the neutral polyhedron built up around Cu1) pile up along the short *a*-axis to form either positively or negatively charged columns in such a way that in the remaining two crystallographic directions (*b* and *c*) an alternating sequence of positively and negatively charged columns is found (Fig. 2).

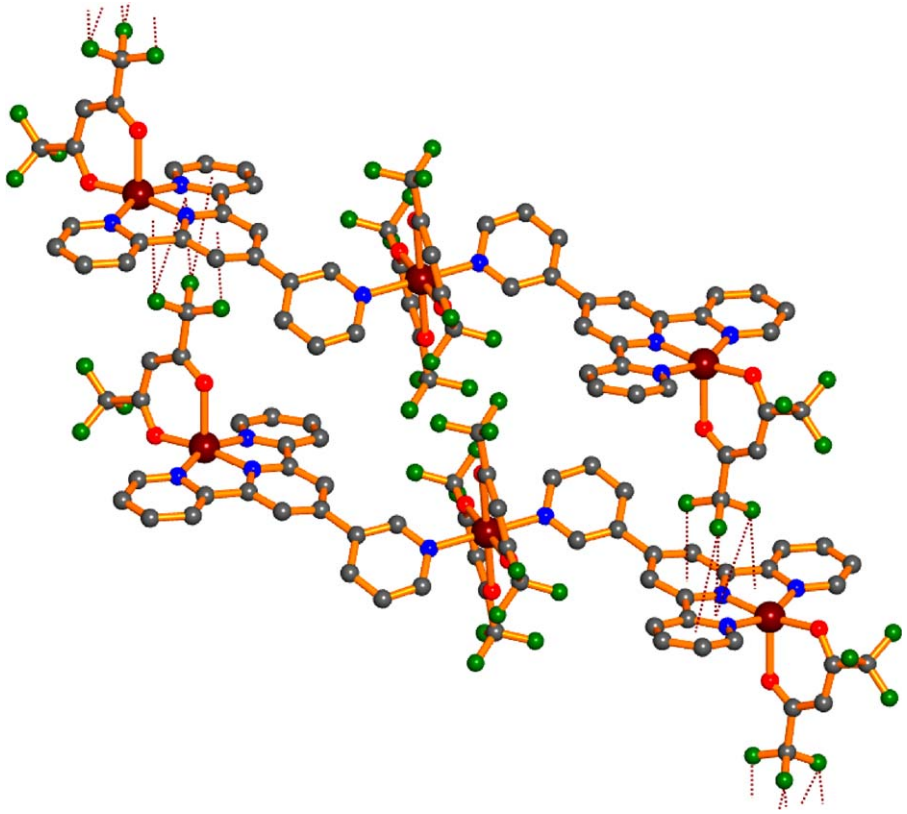

Fig. 3. Packing diagram showing the cation–cation CF/π interactions in **1**. For clarity, hydrogen atoms have been omitted.

2.3. Solid state weak interactions

Despite the prevalence of the coulombian forces in **1**, the crystal packing is notably influenced by the presence of the weak interactions referred as C–F/π, F···F, C–H/F and C–H/O. In this regard, the packing can be rationalized taking into account the pivotal action of the rare C–F/π non-covalent interactions, which are able to connect the ionic species, either of the same or the opposite charge, by using the π-systems provided by five- or six-membered rings. Some CF_3 units in the structure were found disordered with the fluorine atoms over two positions with different degree of occupancy (see Section 4.2); however, in the special cases where C–F/π interactions are present the F atoms appear completely ordered, thus suggesting a stabilizing effect for the interaction.

2.3.1. Intercationic C–F/π interactions

The $[Cu_3(hfacac)_4(\mu\text{-pyterpy})_2]^{2+}$ cations are connected through five C–F/π interactions employing the fluorine atoms of CF_3 groups provided by the hfacac ligand (Fig. 3). The C–F/π interactions are described as C–F···Cg (Cg refers to the ring centroid). They can be classified in two groups based on the π-ring system type: Cg(pyridyl) and Cg(pyridyl-chelate ring) (Table 2). In the first group there are two interactions, F54A···Cg4 and F54B···Cg5, with observed distances of 3.135 and 3.485 Å, respectively. These F···Cg(pyridyl) values agree with the previously communicated interval in organic species containing fluorinated aromatic rings, where the distances $F(CF_3)\cdots Cg(Ar_F)$ span the range 2.996–3.532 Å [20]. It has been suggested that C–F···π(perfluorinated ring) interaction takes place by a contact between the electronegative fluorine and the electropositive centre of the perfluorinated ring [21]. The argument of the positive ring centre is based on its electron density distribution, which is modulated by the fluorine atoms through strong inductive and repulsive electron–electron effects [21,22]. In compound **1**, in the absence of fluorinated rings, the N atoms are expected to exert a modulation to withdraw electron density from heterocycle ring centre.

For the second group of C–F/π interactions, the ring centroids are formulated as Cg(pyridyl-chelate ring) (Table 2). So, these contacts involve the two central five-membered chelate rings (Cg1 and Cg2), and the geometric parameters strongly suggest that an interaction occurs between the CF_3 groups and the chelating pyterpy ligand. Such effect does not seem to have been characterized previously, but its similitude with the above $F(CF_3)\cdots$Cg(pyridyl or Ar_F) assemble is apparent through the comparison of the measured distances (ranging from 3.238 to 3.445 Å, Table 2), and induce us to assume the existence of a similar type of weak contact. Besides, the presence of the two electronegative N atoms on each ring, might be a probable promotion factor for this kind of interactions.

Table 2
C–F···π interactions (Å,°).

C–F···Cg[a,b]	C–F	F···Cg	C···Cg	∠C–F···Cg
(a) Intercations				
Cg(pyridyl)				
C54–F54A···Cg4^{i}	1.311(6)	3.135(5)	3.878(6)	115.1(4)
C54–F54B···Cg5^{i}	1.328(6)	3.485(5)	4.482(7)	131.8(3)
Cg(pyridyl-chelate ring)				
C54–F54C···Cg1^{i}	1.311(6)	3.238(5)	4.171(6)	127.7(4)
C54–F54C···Cg2^{i}	1.311(6)	3.445(5)	3.774(7)	94.2(4)
C54–F54B···Cg2^{i}	1.328(6)	3.415(5)	3.774(7)	95.1(3)
(b) Interanions				
Cg(hfacac-chelate ring)				
C52–F52C···Cg6^{ii}	1.309(6)	3.230(5)	4.035(6)	119.3(3)
(c) Cations–anions				
Cg(pyridyl)				
C12–F12A···Cg3^{ii}	1.278(6)	3.053(5)	4.216(6)	151.0(4)
C53–F53A···Cg5^{iii}	1.305(6)	3.519(5)	4.421(7)	126.5(4)

For atom and Cg labeling see Fig. 1. Symmetry codes: (i) $-1+x, y, z$; (ii) $x, 1+y, z$; (iii) $-x, -1/2+y, 3/2-z$.
[a] Full occupancy F's.
[b] Cg(I) refers to the ring centre-of-gravity.

2.3.2. Interanionic C–F/π interactions

Fig. 4 shows the $[Cu(hfacac)_3]^{-}$ anions connected through a single C–F···π(chelate-hfacac ring) interaction, C52–F52C···Cg6. The distance from the F atom to the centre of the five-membered ring is 3.230 Å and each anion interacts with its upward/downward neighbors to form an infinite 1D network. The similarity of these geometric parameters with those characterizing the above cation–cation interactions (Table 2) and a low electron density on each π-ring centre, due to the presence of two electronegative oxygen atoms together with the inductive effect of the CF_3 groups, suggests that this is a new type of interaction between fluorine atoms and chelate rings with delocalized π-bonds, which to the best of our knowledge has not been informed previously. In the same line of thought, only recently an equivalent approach has

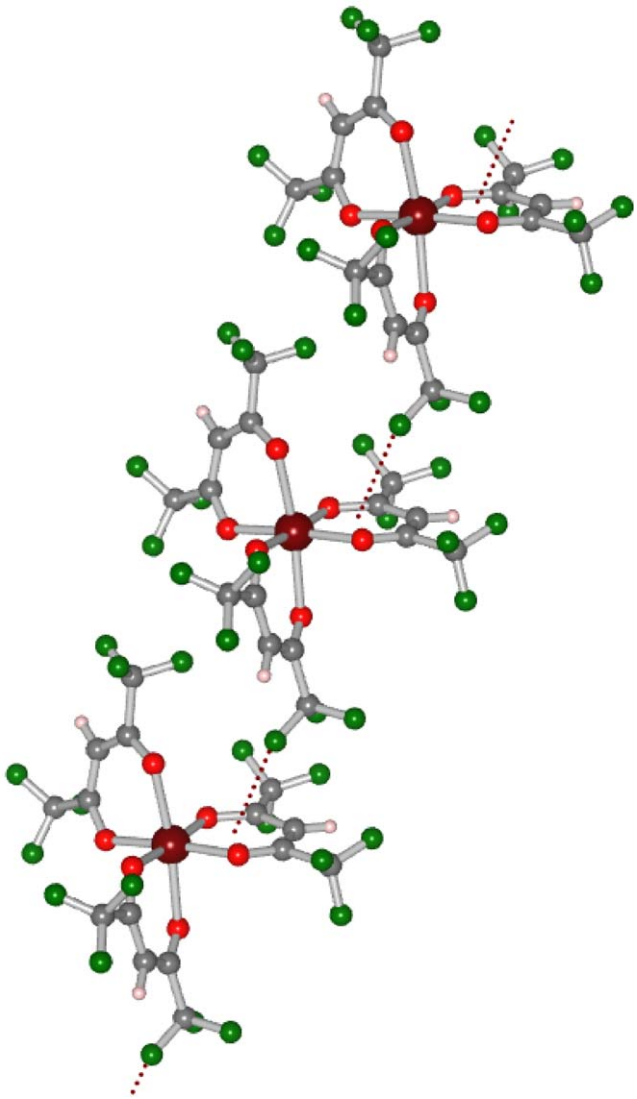

Fig. 4. Packing diagram showing the anion–anion CF/π interactions in **1**.

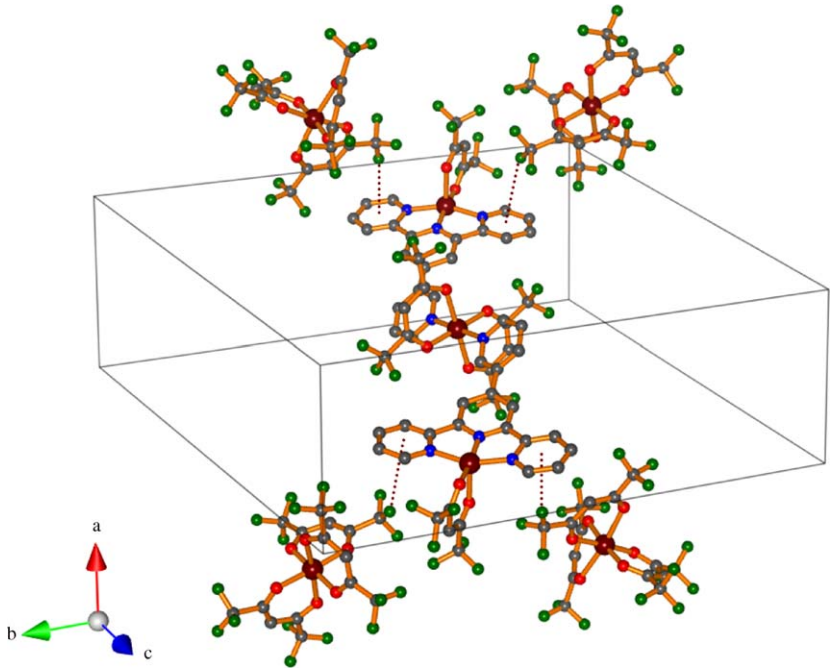

Fig. 5. Packing diagram showing the cation–anion CF/π interactions in **1**. For clarity, hydrogen atoms have been omitted.

been proposed in complexes containing the related chelating acac ligand, in order to evaluate non-covalent interactions of the C–H/π type between H atoms and π-rings of chelating acac ligands [23,24]. But, it must be taken into account the important difference that occurs when the acac ligand is replaced by the hfacac ligand; there is a decrease in the electron density in the π-ring centre, i.e., electron donor CH_3 groups are substituted by electron withdrawing CF_3 groups.

2.3.3. Cation–anion C–F/π interactions

The cations and anions are connected through two C–F···π(pyridyl) interactions, C12–F12A···Cg3 and C53–F53A···Cg5 (Fig. 5), with F···Cg distances of 3.053 and 3.519 Å, respectively. These short distances, quite comparable to those presented for the cation–cation interactions (Table 2), and the presence of N-containing π-rings, constitute the main argument to sustain this interpretation.

2.3.4. F···F interactions

In the present case, there are important C–F···F–C contacts, with fluorine–fluorine distances in some cases significantly shorter than twice the commonly accepted fluorine van der Waals radius R_F ($2 \times R_F$: 2.94 Å) [25], for example F11C···F54B^{i} (i: $-x$, $-0.5 + y$, $1.5 - z$): 2.739(1) Å. This particular interaction links both ion types into some kind of halogen-bonded penta-nuclear unit, and involves precisely the two hfacac groups which display a significant "slanted" coordination (25.2(1)° and 10.5(1)°, respectively). A search in the CSD [12] on non-covalent C–F_3···F_3–C contacts, showed some 8330 cases with the value found in **1** laying in the 12% lowest percentile (Fig. 6); in the absence of any other possible interaction (van der Waal's or otherwise), due to the particular geometry involved, we feel it is safe to ascribe the contact to a genuine F···F interaction. Similar analysis performed on analogous cases in the literature [17–19] confirms that large "slanting" angles are usually correlated to short F···F contacts.

There are, in addition, some other inter-halogen short distances, some of them involve minor components of the disordered sets, spanning a F···F range of 2.78–2.84 Å. Notwithstanding the pre-eminency of coulombian forces in the packing organization, these fluorine–fluorine interactions tend to promote a "bunching" in space (or segregation) effect of fluorine moieties (Fig. 7), a tendency already described in the literature in other fluorinated compounds, and known as "fluorine segregation" [26]. In the absence of stronger interactions, the fluorine segregation can be responsible for packing stabilization. Furthermore, these kind of fluorine···fluorine interactions have been observed in complexes obtained from Cu(hfacac)$_2$ and dipyrrinato-based ligands (F···F range of 2.8–3.6 Å), where an important contribution to the

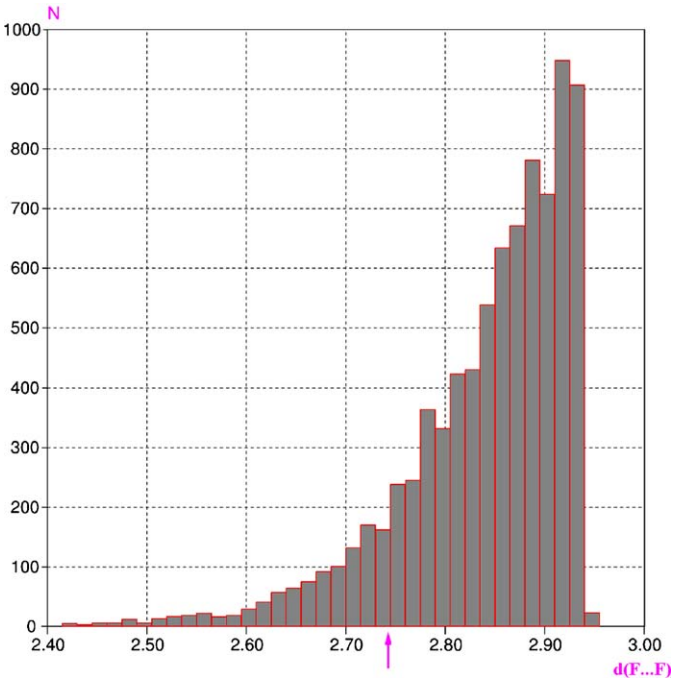

Fig. 6. Histogram of all non-covalent C–F_3···F_3–C distances reported in the CSD [12]. The arrow indicates the value in **1**.

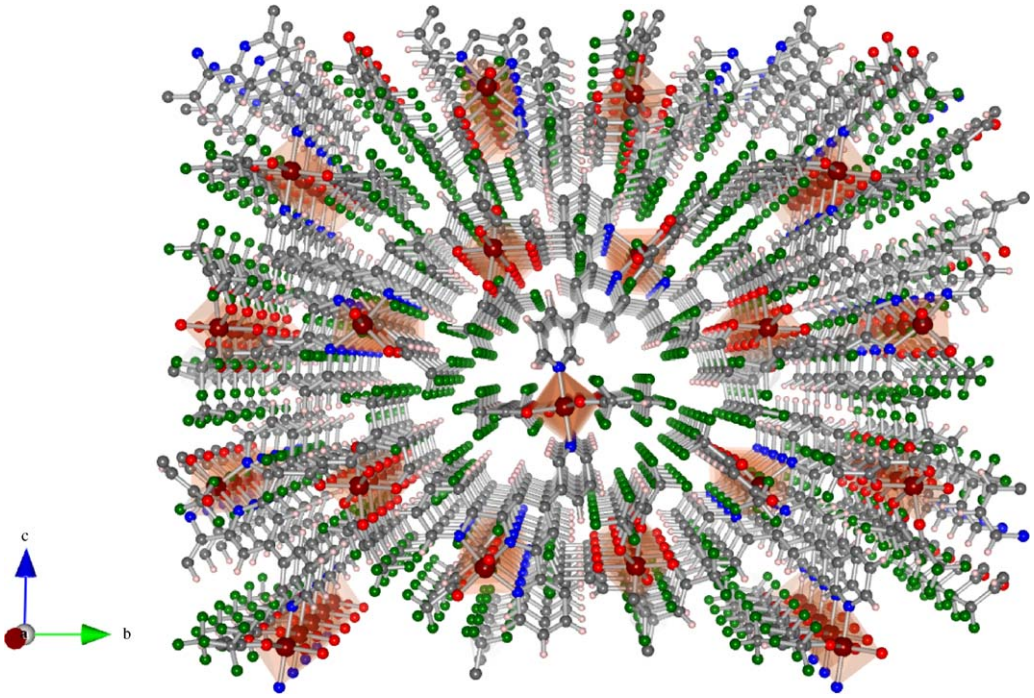

Fig. 7. A projection view of the complex **1** along *a*, showing the fluorine (green) segregation. (For interpretation of the references to color in this figure legend, the reader is referred to the web version of the article.)

topologies of the obtained compounds was attributed to the "self-aggregation" of the fluorine groups [27,28].

In spite of the latter F···F interaction being poorly understood, and the generalized feeling of its extreme weakness [21], there are clear examples in the literature strongly suggesting that the effects of such contacts can be determinant in stabilizing a structure [29].

2.3.5. Hydrogen bond interactions

There are two groups of hydrogen bond interactions: (a) intra-ion and (b) inter-ion (Table 3). The only component of the intra-ion group, C126–H12A···F15B, is located in the cationic trinuclear portion, connecting an outer pyridyl ring of a chelating terpy fragment bonded to Cu2 with a F atom from a hfacac moiety bonded to the central Cu1. The geometric parameters (Table 3, first entry) are close to the range of those observed in the ionic compound $[Co(phen)_2CO_3](Pfbz)\cdot 6H_2O$ (Pfbz = pentafluorobenzoato) (ranges: H···F: 2.538–2.662 Å; C···F: 3.171–3.501 Å; C–H···F: 125.7–150.2°) [30], where it is stated that these type of weak interactions can be discernible despite being ionic species.

In the inter-ion group, both C–H···F and the well established C–H···O contacts coexist. The C–H hydrogen bond donor groups are located on the cation fragment while the F and O atoms are in the anionic species. Distances and angles in the two C–H/F links (Table 3, entries two and three) are also within the above-mentioned ranges. Similarly, the corresponding values in the C–H/O connections (Table 3, entries four to seven), are comparable to those described earlier [31].

Table 3
Hydrogen-bond geometry (Å,°).

D–H···A	H···A	D–H	D···A	∠D–H···A
(a) Intra-ion data				
C126–H12A···F15B[a]	0.96	2.39	3.282(8)	155
(b) Inter-ion data				
C146–H14A···F51C[b]	0.96	2.54	3.438(10)	155
C16–H16A···F52B[b]	0.96	2.50	3.364(9)	151
C136–H13A···O22	0.96	2.55	3.183(7)	124
C176–H17A···O12	0.96	2.50	3.442(8)	168
C46–H46A···O11	0.96	2.57	3.487(7)	161
C76–H76A···O11	0.96	2.51	3.398(6)	154

[a] Full occupancy F's.
[b] Higher occupancy F's.

3. Conclusions

The novel complex $[Cu_3(hfacac)_4(\mu\text{-pyterpy})_2][Cu(hfacac)_3]_2$ has been prepared. The cationic moiety is a trinuclear arrangement with the bridging pyterpy ligand, whereas the mononuclear anionic units are octahedral arrays with the bidentate hfacac species around the metal centre. In spite of the strong ionic coulombian forces, the weak non-covalent interactions, mainly those involving the fluorine atoms, C–H···F, C–F···F–C and C–F···π, are able to control the crystal packing. The key C–F···π type interactions present in the complex are unexpected since they involve π-systems formed by the pyridyl, pyridyl-chelate and hfacac-chelate rings. Consequently, it follows from this work that the central role of this structural effect might be appropriate for the design and synthesis of new materials.

4. Experimental

The solvents were purchased from commercial sources and used without further purification. The compound $Cu(hfacac)_2\cdot H_2O$ was obtained from Aldrich. The pyterpy ligand was prepared according to literature procedures [32]. Infrared spectra were recorded using KBr plates on a Bruker IFS-55 FTIR instrument. Elemental analyses were performed by the CEPEDEQ (Universidad de Chile).

4.1. Synthesis procedure

The complex (**1**) was prepared by reaction between the pyterpy ligand (5.0 mg, 0.016 mmol) and an excess of $Cu(hfacac)_2\cdot H_2O$ (72.0 mg, 0.145 mmol) in CH_2Cl_2 (4.0 mL). The mixture was stirred

Table 4
Crystal data and refinement parameters of **1**.

Empirical formula	$C_{90}H_{38}F_{60}N_8O_{20}Cu_5$
M_w	3008.98 g/mol
Crystal system	Monoclinic
Space group	$P2_1/c$
Unit cell dimensions	a = 8.6921(16) Å, b = 27.470(5) Å, c = 23.913(4) Å, β = 97.861(3)°
V	5656.0(18) Å^3
Z	2
Calculated density	1.767 Mg/m^3
Absorption coefficient (μ)	1.09 mm^{-1}
Reflections (measured/unique/observed)	24,601/10,774/6050
R_{int}	0.087
Data/parameters	11,774/886
R_1, wR_2 [$I > 2\sigma(I)$]	R_1 = 0.074, wR_2 = 0.160
R_1, wR_2 (all data)	R_1 = 0.139, wR_2 = 0.187

to give a clear green solution. Slow evaporation of the solution resulted in well-formed dark green blocks of the complex (**1**). The solid product was washed with CH_2Cl_2 (5× 3.0 mL). Yield: 38.0 mg, 78.9%. Anal. Calcd. for $C_{90}H_{38}F_{60}N_8O_{20}Cu_5$: C, 35.9; H, 1.3; N, 3.7. Found: C, 35.4; H, 1.4; N, 3.7. IR(KBr) (cm^{-1}): 1649, 1529, 1479, 1258, 1202, 1147, 793, 670, 586.

4.2. X-ray crystallography

X-ray data for **1** were recorded at 150K on a Bruker –Smart CCD diffractometer using graphite-monochromated Mo Kα radiation (λ = 0.71073 Å), with SMART-NT [33] as the driving software and SAINT-NT [34] for integration and data reduction. A multi-scan absorption correction was applied using SADABS [35]. The structure was initially solved by direct methods with SHELXS-97 [36] and completed and refined by full-matrix least squares on F2 using the SHELXL-97 [36]. All non-hydrogen atoms were refined with anisotropic thermal parameters. Hydrogen atoms were added at their expected positions (C–H: 0.96 Å) and allowed to ride with a U_H = 1.2 Ueq_{Host}. Six out of the ten C–CF_3 units in the structure presented rotational disorder, and each one was refined with a split model, as two groups having a common C–C vector of full occupancy, and two CF_3 groups with partial occupancies ranging from 0.89/0.11 to 0.76/0.24. These values were allowed to vary in the early stages of refinement, but kept fixed at the end of the process. In order to preserve a meaningful geometry, similarity restraints were applied to C–F, C···F and F···F distances within the same set. A PLATON [37] run in the final stages of refinement revealed four rather small voids in the structure (ca. 70 Å^3 in volume each) with an individual electron content of about 8 electrons, compatible with a minor occupation of some elusive crystal water molecules. The SQUEEZE correction implemented in PLATON [37] was applied to account for the diffuse electron density, though the reported values for F_{000}, density, etc., have been performed using the reported (not the modified) formula. The overall disorder in the structure turned the crystals poorly diffracting, and the reported data set was the best one after inspection of a large number. In spite of the non ideal fraction of reflections gathered up to theta = 50°, reasonable $\#_{reflections}$ to $\#_{parameters}$ ratios were obtained ($n_{tot}/n_{par} > 10$; $n_{gt}/n_{par} \sim 7$).

Data collection and refinement parameters are summarized in Table 4. The molecular representations shown in the figures were generated using XP in the SHELXTL package [36] and VESTA [38]. Crystallographic data (excluding structure factors) for the structures in this paper have been deposited with the Cambridge Crystallographic Data Centre as supplementary publication no. CCDC 749470. Copies of the data can be obtained, free of charge, on application to CCDC, 12 Union Road, Cambridge CB2 1EZ, UK (Fax: +44 1223 336033 or e-mail: deposit@ccdc.cam.ac.uk).

Acknowledgements

The authors acknowledge the Universidad de La Frontera (proyecto DIUFRO No DI09-101) for financial support. We also acknowledge the Spanish Research Council (CSIC) for providing us with a free-of-charge license to the CSD system.

References

[1] E.C. Constable, Chem. Soc. Rev. 36 (2007) 246–253.
[2] I. Eryazici, Ch.N.G. Moorefield, R. Newkome, Chem. Rev. 108 (2008) 1834–1895.
[3] H. Feng, X.-P. Zhou, T. Wu, D. Li, Y.-G. Yin, S.W. Ng, Inorg. Chim. Acta 359 (2006) 4027–4035.
[4] L. Gou, B. Zhang, H.-M. Hu, X.-L. Chen, B.-Ch. Wang, Q.-R. Wu, T. Qin, Z.-X. Tang, J. Mol. Struct. 889 (2008) 244–250.
[5] L. Gou, Q.-R. Wu, H.-M. Hu, T. Qin, G.-L. Xue, M.-L. Yang, Z.X. Tang, Polyhedron 27 (2008) 1517–1526.
[6] L. Gou, L.-F. Xu, H.-M. Hu, B.-C. Wang, Q.-R. Wu, X.-L. Chen, Z.-X. Tang, Z. Anorg, Allg. Chem. 634 (2008) 1215–1220.
[7] C.M. Ollagnier, D. Nolan, C.M. Fitchett, S.M. Draper, Inorg. Chem. Commun. 10 (2007) 1045–1048.
[8] S.-S. Sun, A.S. Silva, I.M. Brinn, A.J. Lees, Inorg. Chem. 39 (2000) 1344–1345.
[9] S.-S. Sun, A.J. Lees, Inorg. Chem. 40 (2001) 3154–3160.
[10] S. Hayami, K. Hashiguchi, G. Juhász, M. Ohba, H. Okawa, Y. Maeda, K. Kato, K. Osaka, M. Takata, K. Inoue, Inorg. Chem. 43 (2004) 4124–4126.
[11] L. Hou, D. Li, W.J. Shi, Y.-G. Yin, S.W. Ng, Inorg. Chem. 44 (2005) 7825–7832.
[12] F.H. Allen, Acta Crystallogr. B 58 (2002) 380–388.
[13] V. Pawlowski, H. Kunkely, M. Zabel, A. Vogler, Inorg. Chim. Acta 357 (2004) 824–826 (CSD entry ISIPIJ).
[14] M.R. Truter, B.L. Vickery, J. Chem. Soc., Dalton Trans. (1972) 395–403 (CSD entry NAFACU10).
[15] A. Okazawa, T. Ishida, T. Nogami, Polyhedron 24 (2005) 2584–2587 (CSD entry LEBJAE).
[16] P. Tasker, A. Parkin, C. Squires, S. Parsons, D. Messenger, Private Communication to the CSD, 2005 (CSD entry QASFIA).
[17] (a) L.S. von Chrzanowski, M. Lutz, A.L. Spek, Acta Crystallogr. C 63 (2007) m283–m288 (CSD entry COACAC06);
(b) L.S. von Chrzanowski, M. Lutz, A.L. Spek, Acta Crystallogr. C 63 (2007) m377–m382 (CSD entry ACACCR08).
[18] S. Geremia, N. Demitri, J. Chem. Educ. 82 (2005) 460–465 (CSD entry ACACMN23).
[19] I. Diaz-Acosta, J. Baker, W. Cordes, P. Pulay, J. Phys. Chem. A 105 (2001) 238–244 (CSD entry FEACAC05).
[20] I.Y. Bagryanskaya, M.A. Grishina, L.Y. Safina, G.A. Selivanova, V.A. Potemkin, Y.V. Gatilov, J. Struct. Chem. 49 (2008) 901–908.
[21] K. Reichenbächer, H.I. Süss, J. Hulliger, Chem. Soc. Rev. 34 (2005) 22–30.
[22] P. Politzer, J.W. Timberlake, J. Org. Chem. 37 (1972) 3557–3559.
[23] M.K. Milčić, V.B. Medaković, D.N. Sredojević, N.O. Juranić, S.D. Zarić, Inorg. Chem. 45 (2006) 4755.
[24] J. Granifo, M. Vargas, M.T. Garland, A. Ibañez, R. Gaviño, R. Baggio, Inorg. Chem. Commun. 11 (2008) 1388–1391.
[25] A. Bondi, J. Phys. Chem. 48 (1964) 441.
[26] O. Jeannin, M. Fourmigué, C.R. Chim. 9 (2006) 1287–1294.
[27] S.R. Halper, S.M. Cohen, Angew. Chem. Int. Ed. 43 (2004) 2385–2388.
[28] S.R. Halper, S.M. Cohen, Inorg. Chem. 44 (2005) 4139–4141.
[29] M.D. Prasanna, T.N. Guru Row, J. Mol. Struct. 562 (2001) 55–61.
[30] A. Singh, R.P. Sharma, T. Aree, P. Venugopalan, J. Fluorine Chem. 130 (2009) 650–655.
[31] G.R. Desiraju, Acc. Chem. Res. 29 (1996) 441–449.
[32] J.E. Beves, E.L. Dunphy, E.C. Constable, C.E. Housecroft, C.J. Kepert, M. Neuburger, D.J. Price, S. Schaffner, Dalton Trans. (2008) 386–396.
[33] Bruker, SMART-NT, V5, Data Collection Software, Siemens Analytical X-ray Instruments Inc., Madison, WI, USA, 2001.
[34] Bruker, SAINT-NT, V6, Data Reduction Software, Siemens Analytical X-ray Instruments Inc.,, Madison, WI, USA, 2002.
[35] G.M. Sheldrick, SADABS, Multiscan Absorption Correction Program, University of Göttingen, Germany, 2001.
[36] G.M. Sheldrick, SHELXL-97, SHELXS-97, SHELXTL, Acta Crystallogr. A 64 (2008) 112–122.
[37] A.L. Spek, J. Appl. Crystallogr. 36 (2003) 7–13.
[38] K. Momma, F. Izumi, VESTA: a three-dimensional visualization system for electronic and structural analysis, J. Appl. Crystallogr. 41 (2008) 653–658.